Int. J. Solids Structures, 1971, Vol. 7, pp. 473 to 493. Pergamon Press. Printed in Great Britain

NATURAL FREQUENCIES AND ELASTIC STABILITY OF A SIMPLY-SUPPORTED RECTANGULAR PLATE UNDER LINEARLY VARYING COMPRESSIVE LOADS

G. FAUCONNEAU† and R. D. MARANGONI†

201 Engineering Hall, University of Pittsburgh, Pittsburgh, Pennsylvania 15213

Abstract—The effects of constant edge loads and of a uniformly distributed in-plane load on the transverse vibrational frequencies and elastic stability characteristics of a simply-supported plate are investigated. Bounds for the eigenvalues are obtained for various plate width-to-length ratios as functions of two parameters associated with the distributed in-plane load and the edge loads. The upper bounds are calculated by the Rayleigh–Ritz method and the lower bounds by the Second Projection Method of Bazley and Fox. In all instances, the gap between the bounds over their average is less than $\frac{1}{2}$ per cent. Buckling load combinations are obtained by determining the values of the loading parameters making the first eigenvalue equal to zero.

NOTATION

Latin symbols

a	length of the plate
a_{ij}	matrix elements [equation (46)]
b	width of the plate
c_i	constants of linear combination [equation (20)]
D	flexural rigidity of the plate
$D_L, D_L^0, D_{L'}$	respective domains of the operators L, L^0 and L'
f	function of class C^4 defined over $0 \leq x \leq 1$ [equation (16)]
G	function of time [equation (6)]
g	function of class C^4 defined over $0 \leq x \leq 1$ [equation (16)]
g	acceleration due to gravity
H	Hilbert space
J_0, J_1	Bessel functions of the first kind of orders zero and one
$j_{0,i}$	zeros of $J_0(x)$
L	differential operator in eigenvalue problem [equation (13)]
L^0	base operator [equation (27)]
L'	additional operator [equation (28)]
$L^k, L^{l,k}$	intermediate operators
m	plate density per unit area
N_x, N_y, N_{xy}	in-plane loads per unit of length
P_1	compressive thrust per unit of length at the edge $x = 0$
P_{cr}	uniform critical compressive load for a simply supported plate
$\mathbf{P}^k$	projection operator [equation (36)]
Q^l	projection operator [equation (44)]
r	aspect ratio of the plate [equation (12)]
t	time
u	function in the domain of L
u_i	function in D_L [equation (23)]
v	function in D_L [equation (17)]
$\bar{w}$	lateral deflection of the plate [equation (1)]
X	body force component per unit area

† Associate Professor of Mechanical Engineering.

$\bar{x}$	actual coordinate
x	non-dimensional coordinate $x = \bar{x}/a$
Y	body force component per unit area
y	actual coordinate
$\bar{y}$	non-dimensional coordinate $y = \bar{y}/b$

Greek symbols

α	distributed in-plane load parameter [equation (12)]
α_i	constants of linear combination [equation (44)]
β	parameter [equation (12)]
β_i	constants of linear combination [equation (59)]
γ	edge load parameter [equation (12)]
γ^*	positive number [equation (42)]
δ_{ij}	Kronecker delta
ε	circular frequency of vibration [equation (7)]
$\phi(\bar{x}, \bar{y})$	mode shape of deflection [equation (6)]
ϕ	function
$\psi(x)$	eigenfunction of the operator L [equation (11)]
ψ_i^0	eigenfunction of the operator L^0 [equation (30)]
ψ_i'	eigenfunction of the operator L' [equation (40)]
$\psi^{l,k}$	eigenfunction of the operator $L^{l,k}$ [equation (56)]
λ_i	eigenvalue of the operator L [equation (13)]
$\bar{\lambda}_i$	upper bound for the eigenvalue
λ_i^0	eigenvalue of the operator L^0 [equation (30)]
λ_i'	eigenvalue of the operator L' [equation (41)]
$\lambda_i^{l,k}$	eigenvalue of the intermediate operator $L^{l,k}$ [equation (56)]

1. INTRODUCTION

FOR many heavily loaded structural elements used in aerospace applications, inertia forces are of great significance. For instance, the body forces developed in the mid-plane of a plate by an acceleration component in this plane affect the potential energy of the plate and, consequently, its natural frequencies of vibration and its stability characteristics.

The effect of in-plane loads on the deflection, natural frequencies and buckling stresses for plates appears to have been considered mainly for the case where these loads are uniform throughout the plate.

Bickley [1] considered a clamped circular plate under tension and investigated the effect of this tension on the normal displacements under pressure, and on the natural frequencies of the plate.

Conway and his associates [2–4] determined the effect of combinations of uniform tensile or compressive in-plane loads on the deflection and stress distribution of simply supported and clamped rectangular plates.

Stein and Neff [5] determined the buckling stresses for a simply supported rectangular plate in shear using the Rayleigh–Ritz method, while McKenzie [6] considered the buckling of a rectangular plate under combined bi-axial compression, bending and shear with two edges simply supported while the other two edges were arbitrarily supported. His solution was obtained by an approximate variational method.

Johns [7] determined the static instability of rectangular orthotropic panels subjected to bi-axial in-plane compression and lateral loads dependent on the panel deflection. The panels were considered to be resting on an elastic foundation and their edges were elastically restrained against rotation.

Wang and Sussman [8] considered the elastic stability of a simply supported plate under linearly variable compressive loads. Using the Rayleigh–Ritz method, they determined the buckling coefficients and presented them in graphical form for different length-to-width ratios. They concluded that the average buckling stress in the plate is less than the uniform buckling stress and that the body force is a contributing factor to the compressive stresses.

Weeks and Shideler [9] investigated the effect of constant bi-axial in-plane loads on the vibration characteristics of rectangular plates with various boundary conditions. Their solutions are exact if one pair of opposite edges is simply supported, otherwise the solutions are approximate.

Further results for rectangular plates subjected to uniform in-plane loads can be found in Refs. [10–12], and in Refs. [13 and 14] for skew plates.

Herrmann [15] appears to be the only author having considered the effect of a body force and uniaxial in-plane compression on the fundamental frequency of vibration of a simply supported rectangular plate. The body force acting in the plane of the plate may be due to its weight or to an acceleration of the plate in its plane. Using the Rayleigh method, Herrmann calculated an approximation to the fundamental frequency and to the buckling load for a plate with aspect ratio equal to 3. As a first approximation, the linear term was replaced by its average. The frequency decrease was found to be piecewise linear with increasing fractions of the critical loading.

In summary, one finds that in nearly all the cases treated in the literature, the in-plane loads have been taken as being constant, and that in the only two instances where the body force has been considered the effect of the distributed load on the buckling load and on the fundamental frequency is obtained by approximate techniques.

The object of the present investigation is then to determine the effect of a linearly varying compressive load on the natural frequencies of a simply supported rectangular plate, taking into account the influence of the plate aspect ratio. The type of loading considered here gives rise to a differential equation with variable coefficients whose solution is difficult to obtain. In order to find approximate solutions, two methods are used:

The Rayleigh–Ritz method is utilized to calculate upper bounds for the natural frequencies. However, since the *quality* of these upper bounds is unknown without calculations of error estimates or, what is equivalent, of lower bounds, the Second Projection method of Bazley and Fox [16] is used to complete the prediction of the frequencies. Brief descriptions of these mathematical methods are given in Section 3.

The determination of the buckling loads is accomplished by finding the values of the loading parameters for which the first eigenvalue of the plate goes to zero. Some of the results obtained here are compared to the results of Wang and Sussman [8].

Section 2 is concerned with the derivation of the plate eigenvalue problem for the determination of the plate natural frequencies, and the results are presented and discussed in Section 4.

2. FORMULATION OF THE PROBLEM

Consider a rectangular plate having uniform thickness, h, small in comparison to its length a in the $\bar{x}$-direction and its width b in the $\bar{y}$-direction.

The plate is subjected to in-plane loads N_x, N_y, N_{xy} given per unit of length, and to body forces X and Y given per unit area and acting in the middle plane.

The differential equation governing the lateral deflection $\bar{w}(\bar{x}, \bar{y}, t)$ of the plate can readily be obtained from Ref. [11, p. 335] by inclusion of the inertia term. In the absence of lateral loads, it reads

$$m\frac{\partial^2 \bar{w}}{\partial t^2}+D\nabla^4\bar{w}-N_x\frac{\partial^2 \bar{w}}{\partial \bar{x}^2}-N_y\frac{\partial^2 \bar{w}}{\partial \bar{y}^2}-2N_{xy}\frac{\partial^2 \bar{w}}{\partial \bar{x}\partial \bar{y}}+X\frac{\partial \bar{w}}{\partial \bar{x}}+Y\frac{\partial \bar{w}}{\partial \bar{y}}=0 \tag{1}$$

where m denotes the plate density per unit area and D is the flexural rigidity

$$D=\frac{Eh^3}{12(1-\nu^2)}. \tag{2}$$

The in-plane loads must satisfy the equilibrium equations

$$\begin{aligned}\frac{\partial N_x}{\partial \bar{x}}+\frac{\partial N_{xy}}{\partial \bar{y}}+X&=0\\ \frac{\partial N_{xy}}{\partial \bar{x}}+\frac{\partial N_y}{\partial \bar{y}}+Y&=0.\end{aligned} \tag{3}$$

For the plate subjected to a uniform compressive thrust P_1, along the edge $\bar{x}=0$ and to a distributed body force mg per unit area, the in-plane loads are given by

$$N_x=-[P_1+mg\bar{x}], \qquad N_x=N_{xy}=0, \qquad X=mg, \qquad Y=0. \tag{4}$$

The loading and the geometry are illustrated in Fig. 1. That such a state of stress is possible can be seen by substitution of these expressions in the equilibrium equations (3). However, this stress distribution involves the assumption that the plate is free to deform in its own plane.

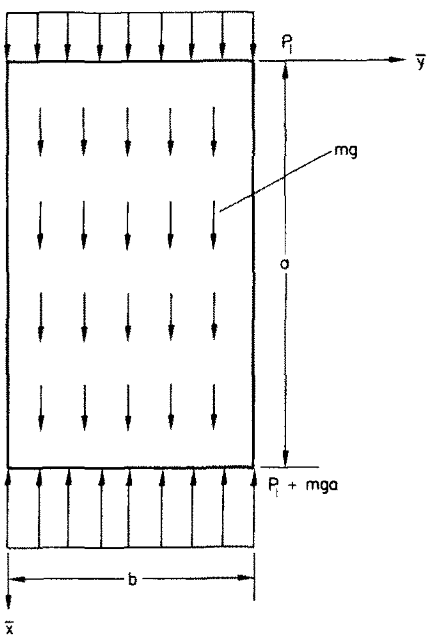

FIG. 1. Plate subjected to linearly varying compressive loads.

Upon substitution of the in-plane loads (4) into equation (1), the lateral deflection of the plate is governed by

$$m\frac{\partial^2\bar{w}}{\partial t^2}+D\nabla^4\bar{w}+(P_1+mg\bar{x})\frac{\partial^2\bar{w}}{\partial\bar{x}^2}+mg\frac{\partial\bar{w}}{\partial\bar{x}} = 0. \tag{5}$$

The search for eigenvibrations of the form

$$\bar{w}(\bar{x},\bar{y},t) = \phi(\bar{x},\bar{y})G(t) \tag{6}$$

yields the pair of equations

$$\frac{\mathrm{d}^2G}{\mathrm{d}t^2}+\varepsilon^2G = 0 \tag{7}$$

$$\nabla^4\phi+\frac{1}{D}(P_1+mg\bar{x})\frac{\partial^2\phi}{\partial\bar{x}^2}+\frac{mg}{D}\frac{\partial\phi}{\partial\bar{x}}-\frac{m\varepsilon^2\phi}{D} = 0 \tag{8}$$

where ε^2, the separation constant, represents the square of the circular frequency of the motion.

At this stage, separation of the variables $\bar{x}$ and $\bar{y}$ can be accomplished only if the plate is simply supported along the edges $\bar{y} = 0$ and $\bar{y} = b$. In this case, ϕ can be written in the form,

$$\phi(\bar{x},\bar{y}) = \psi(x)\underline{\Omega}(y) \tag{9}$$

where $x = \bar{x}/a$ and $y = \bar{y}/b$ and

$$\underline{\Omega}_n(y) = C_n\sin n\pi y \tag{10}$$

while ψ must satisfy the differential equation

$$\frac{\mathrm{d}^4\psi}{\mathrm{d}x^4}+\left(\frac{P_1a^2}{D}+\frac{mga^3x}{D}-\frac{2n^2\pi^2a^2}{b^2}\right)\frac{\mathrm{d}^2\psi}{\mathrm{d}x^2}+\frac{mga^3}{D}\frac{\mathrm{d}\psi}{\mathrm{d}x}-\left(\frac{m\varepsilon^2a^4}{D}-\frac{n^4\pi^4a^4}{b^4}\right)\psi = 0. \tag{11}$$

Introduction of the parameters

$$\alpha = mga^3/D$$
$$a/b = r$$
$$\gamma = P_1/P_{\mathrm{cr}} = P_1b^2/k\pi^2D$$

where k is a numerical factor depending on r as defined by Timoshenko and Gere [11],

$$\begin{aligned}\beta &= \frac{\pi^2}{\alpha}[k\gamma r^2-2(nr)^2]\\ \lambda &= a^4\left[\frac{\varepsilon^2m}{D}-\frac{n^4\pi^4}{b^4}\right]\end{aligned} \tag{12}$$

permits equation (11) to be written in the form

$$\frac{\mathrm{d}^4\psi}{\mathrm{d}x^4}+\alpha\frac{\mathrm{d}}{\mathrm{d}x}\left[(\beta+x)\frac{\mathrm{d}\psi}{\mathrm{d}x}\right] = \lambda\psi \tag{13}$$

with the boundary conditions (for simple supports at $\bar{x} = 0$ and $\bar{x} = a$):

$$\psi = \frac{d^2\psi}{dx^2} = 0 \quad \text{at } x = 0 \text{ and } x = 1. \tag{14}$$

The solution of equation (13) with boundary conditions (14) constitute the eigenvalue problem to be solved. The natural frequencies of the plate are related to the eigenvalues λ by the relation

$$\varepsilon_{pq}^2 = \frac{D}{ma^4}\left[\lambda_p + \frac{q\pi^4\alpha^4}{b^4}\right] \tag{15}$$

where p and q give the mode of vibration, i.e. the numbers of half waves in which the vibrating plate deforms in the $\bar{x}$ and $\bar{y}$ directions respectively.

The determination of the buckling loads will be discussed in Section 4. Presently attention will be restricted to the determination of the upper and lower bounds to the natural frequencies, i.e. to the bounds to the eigenvalues specified by equations (13) and (14). It should be noted that an eigenvalue problem of the form found here was considered previously by one of the authors in a different application [17].

To establish the basis for the estimation of the eigenvalues λ, the mathematical problem will be cast in variational form.

The differential operator appearing in equation (13), and henceforth denoted by L, has a domain D_L consisting of the set of functions of class C^4 defined over the range $0 \leq x \leq 1$ and satisfying the boundary conditions (14). Over this range, the inner product between two functions f and g is denoted by and given by the Lebesgue integral

$$(f, g) = \int_0^1 f(x)g(x)\,dx. \tag{16}$$

It can be shown by integration by parts that the operator L is self-adjoint, i.e.

$$(Lu, v) = (u, Lv) \tag{17}$$

for any two functions u and v in D_L.

Now, as is well known, a variational principle can always be constructed from a self-adjoint operator in such a way that the corresponding Euler equation is the given differential equation. If we assume that the eigenvalues of L are ordered in the non-decreasing sequence

$$\lambda_1 \leq \lambda_2 \leq \lambda_3 \leq \ldots. \tag{18}$$

Courant's maximum–minimum principle [18] gives the following characterization for the jth eigenvalue:

$$\lambda_j = \max_{\{u_i\}}\left\{\min_{(\phi,u_i)=0} \frac{\int_0^1 [(d^2\phi/dx^2)^2 - \alpha(\beta+x)(d\phi/dx)^2]\,dx}{\int_0^1 \phi^2\,dx}\right\}_{i=1 \text{ to } j-1} \tag{19}$$

where ϕ and the set of functions $\{u_i\}$ belong to D_L.

The problem is now reduced to finding approximations to the stationary values of the Rayleigh quotient shown in equation (19).

3. DISCUSSION OF THE SOLUTION

The number and variety of techniques that have been used to estimate eigenvalues of self-adjoint operators is enormous. For review of the literature on this subject, the reader is referred to Refs. [19–22].

The methods used here to bracket the eigenvalues are the Rayleigh–Ritz method and the Second Projection method of Bazley and Fox [16].

(a) *Upper bounds (Rayleigh–Ritz method)*

The central idea in the Rayleigh–Ritz method consists in determining the stationary values of the Rayleigh quotient over the linear manifold spanned by a set of n linearly independent functions $\{u_i\}$ satisfying the prescribed boundary conditions of the operator L. The problem consists, then, in finding the functions u of the form

$$u = \sum_{i=1}^{n} c_i u_i \tag{20}$$

i.e. in finding the constants c_i, making the quotient stationary, and its corresponding value. The result is the general matrix eigenvalue problem

$$[(u_i, Lu_j)][c_j] = \hat{\lambda}[(u_i, u_j)][c_j]. \tag{21}$$

Now since the set of functions u was restricted to the finite-dimensional manifold, it is apparent that the eigenvalues $\hat{\lambda}_j$ are upper bounds to the eigenvalues of the operator L, i.e.

$$\hat{\lambda}_j \geq \lambda_j, \qquad j = 1, 2, \ldots n \tag{22}$$

Furthermore, it follows that as n increases, the upper bounds will be improved since the Rayleigh quotient will take its stationary value over a larger subspace.

In the present study, the functions u_i were chosen as follows:

$$u_i = \sqrt{2}\sin i\pi x. \tag{23}$$

They are orthonormal, i.e.

$$(u_i, u_j) = \delta_{ij} \tag{24}$$

and they yield the following inner products:

$$\begin{aligned}(u_i, Lu_j) &= 0 && \text{for } (i \pm j) \text{ even} \\ &= 2\alpha ij\left[\frac{1}{(i-j)^2}+\frac{1}{(i+j)^2}\right] && \text{for } (i \pm j) \text{ odd} \\ &= (i\pi)^2[(i\pi)^2-\alpha\beta-\tfrac{1}{2}\alpha] && \text{for } i = j.\end{aligned} \tag{25}$$

The inner products were used to solve numerically the matrix eigenvalue problem specified by equation (21). The results are presented and discussed in Section 4.

(b) *Lower bounds (Bazley–Fox Second Projection method)*

In the determination of lower bounds of a self-adjoint operator L, the method of intermediate problems introduced by Weinstein and Aronszajn [20] was modified by Bazley and Fox by the introduction of a second projection in order to reduce their determination to finite, linear algebraic computations. Only the outline of the method will be given here. For further details and proofs, the reader is referred to Ref. [16].

We consider the set of all square integrable functions defined on the interval [0, 1] along with the inner product defined in equation (16). This set, along with the inner product defined, constitutes a separable Hilbert space which will be denoted by H. The self-adjoint operator L in H is assumed to be decomposable as the sum of two operators

$$L = L^0 + L' \tag{26}$$

where L^0 is a self-adjoint operator with easily solved eigenvalue problem and L' is positive definite and self-adjoint.

We take for L^0 the operator

$$L^0 = \frac{d^4}{dx^4} + \alpha(\beta+1)\frac{d^2}{dx^2} \tag{27}$$

and for L'

$$L' = -\frac{d}{dx}\left[\alpha(1-x)\frac{d}{dx}\right] \tag{28}$$

L^0 is easily shown to be self-adjoint, and its eigenvalue problem, viz.

$$\begin{aligned} &\frac{d^4\psi^0}{dx^4} + \alpha(\beta+1)\frac{d^2\psi_0}{dx^2} = \lambda^0\psi^0 \\ &\psi^0 = \frac{d^2\psi^0}{dx^2} = 0 \quad \text{at } x = 0 \text{ and } x = 1 \end{aligned} \tag{29}$$

has the solution

$$\psi_n^0 = \sqrt{2}\sin n\pi x$$

and

$$\lambda_n^0 = (n\pi)^2[(n\pi)^2 - \alpha(\beta+1)]. \tag{30}$$

The domain of L', $D_{L'}$, consists of the set of functions of class C^2 vanishing at $x = 0$ and $x = 1$. For any function ϕ in $D_{L'}$,

$$(L'\phi, \phi) = -\int_0^1 \frac{d}{dx}\left[\alpha(1-x)\frac{d\phi}{dx}\right]\phi\, dx = \int_0^1 \alpha(1-x)\left(\frac{d\phi}{dx}\right)^2 dx - \left[\alpha(1-x)\phi\frac{d\phi}{dx}\right]_0^1 \tag{31}$$

Since the boundary term vanishes,

$$(L'\phi, \phi) > 0 \quad \text{for } \phi \neq 0 \tag{32}$$

i.e. L' is positive definite. Furthermore, it can be shown by integration by parts that L' is self-adjoint. Now since L' is non-negative and D_L coincides with D_{L^0},

$$(u, L^0u) \leq (u, Lu) \tag{33}$$

and consequently the ordered eigenvalues of L^0 and L satisfy the inequalities:

$$\lambda_i^0 \leq \lambda_i \qquad i = 1, 2, 3 \ldots. \tag{34}$$

Thus the eigenvalues of L^0 are lower bounds to those of L. However, in most instances (including in this application) these lower bounds are far removed from the true eigenvalues λ_i. In order to improve these rough bounds, a sequence of self-adjoint operators L^k is constructed so that they have the same domain as L^0 and their eigenvalues satisfy the inequalities

$$\lambda_i^0 \le \lambda_i^k \le \lambda_i^{k+1} \le \lambda_i. \tag{35}$$

In the Weinstein–Aronszajn construction, the intermediate operators L^k are constructed using linearly independent vectors in $D_{L'}$. Here, we select as these vectors the eigenfunctions ψ_i' of the operator L'. The projection of any function ϕ in $D_{L'}$ on the span of the first k eigenfunctions of L' is given by

$$\mathbf{P}^k\phi = \sum_{i=1}^{k} (\phi, \psi_i')\psi_i' \tag{36}$$

The kth operator L^k is then defined by

$$L^k\phi = L^0\phi + L'\mathbf{P}^k\phi = L^0\phi + \sum_{i=1}^{k} (\phi, \psi_i')L'\psi_i'. \tag{37}$$

Its domain is D_{L^0} and it is self-adjoint as can easily be shown. The inequalities

$$(\phi, L^0\phi) \le (\phi, L^k\phi) \le (\phi, L^{k+1}\phi) \le (\phi, L\phi) \tag{38}$$

being satisfied, the parallel inequalities (35) are also satisfied. The determination of the eigenfunctions ψ_i' requires the solution of the eigenvalue problem

$$-\frac{\mathrm{d}}{\mathrm{d}x}\left[\alpha(1-x)\frac{\mathrm{d}\psi'}{\mathrm{d}x}\right] = \lambda'\psi' \tag{39}$$

with

$$\psi'(0) = \psi'(1) = 0.$$

The normalized eigenfunctions for this problem are

$$\psi_i' = \frac{1}{J_1(j_{0,i})} J_0[j_{0,i}\sqrt{(1-x)}] \tag{40}$$

where J_0 and J_1 are respectively the Bessel functions of the first kind of order zero and one, and $j_{0,i}$ are the zeros of $J_0(x)$. The corresponding eigenvalues are

$$\lambda_i' = \frac{\alpha j_{0,i}^2}{4}. \tag{41}$$

It is readily apparent that the determination of the spectrum of the intermediate operator L^k gives lower bounds to those of L. In general, however, the eigenvalue problem for L^k presents difficulties, and in order to overcome them, Bazley and Fox [16] have modified the intermediate operator L^k by introducing smaller operators $L^{l,k}$ whose spectra can always be determined by finite algebraic computations.

For every positive number γ^*, the operator L^k may be written as

$$L^k = (L^0 - \gamma^*) + (L'\mathbf{P}^k + \gamma^*). \tag{42}$$

Consider the inner product $\langle u, v\rangle$ defined for any two functions u and v of H by

$$\langle u, v\rangle = ([L'\mathbf{P}^k + \gamma^*]u, v). \tag{43}$$

Consider a set $\{q_i\}$ of linearly independent functions in H. The projection Q^l of an element ϕ of H on the linear manifold spanned by the first l vectors of the set is given by

$$Q^l\phi = \sum_{i=1}^{l} \alpha_i q_i \tag{44}$$

where

$$\alpha_i = \sum_{j=1}^{l} a_{ij}(\phi, [L'\mathbf{P}^k+\gamma^*]q_j) \tag{45}$$

and where the a_{ij} are the elements of the matrix inverse to that with $\langle q_i, q_j\rangle$, i.e.

$$[a_{ij}] = [([L'\mathbf{P}^k+\gamma^*]q_i, q_j)]^{-1}. \tag{46}$$

Hence the projection $Q^l\phi$ can be written as

$$Q^l\phi = \sum_{i=1}^{l}\sum_{j=1}^{l} a_{ij}(\phi, [L'\mathbf{P}^k+\gamma^*]q_j)q_i \tag{47}$$

As l increases, the projection $Q^l\phi$ increases, and for any ϕ in H,

$$0 \le (\phi, [L'\mathbf{P}^k+\gamma^*]Q^l\phi) \le (\phi, [L'\mathbf{P}^k+\gamma^*]Q^{l+1}\phi) \le (\phi, [L'\mathbf{P}^k+\gamma^*]\phi). \tag{48}$$

The operators $L^{l,k}$ are now defined by

$$L^{l,k} = [L^0-\gamma^*]+[L'\mathbf{P}^k+\gamma^*]Q^l. \tag{49}$$

They have the explicit representation

$$L^{l,k}\phi = [L^0-\gamma^*]\phi+\sum_{i=1}^{l}\sum_{j=1}^{l} a_{ij}(\phi, [L'\mathbf{P}^k+\gamma^*]q_j)[L'\mathbf{P}^k+\gamma^*]q_i. \tag{50}$$

In view of equations (48) and (50) we have

$$(\phi, [L^0-\gamma^*]\phi) \le (\phi, L^{l,k}\phi) \le (\phi, L^{l+1,k}\phi) \le (\phi, L^k\phi) \le (\phi, L\phi) \tag{51}$$

for any ϕ in D_L, and the corresponding eigenvalues satisfy then the parallel inequalities

$$\lambda_i^0-\gamma^* \le \lambda_i^{l,k} \le \lambda_i^{l+1,k} \le \lambda_i^k \le \lambda_i. \tag{52}$$

The original problem now reduces to the solution of the eigenvalue problem

$$L^{l,k}\psi = \lambda^{l,k}\psi \tag{53}$$

for the determination of lower bounds to the eigenvalues of the operator L.

To facilitate the solution of this problem, the following special choice of the functions q_i can always be made:

$$q_i = [L'\mathbf{P}^k+\gamma^*]^{-1}\psi_i^0 \tag{54}$$

where ψ_i^0 are the eigenfunctions of L^0 given by equation (30). With this choice, the operator $L^{l,k}$ takes the form

$$L^{l,k}\phi = [L^0-\gamma^*]\phi+\sum_{i=1}^{l}\sum_{j=1}^{l} a_{ij}(\phi, \psi_i^0)\psi_j^0 \tag{55}$$

and the eigenvalue problem under consideration becomes

$$L^{l,k}\psi^{l,k} = [L^0-\gamma^*]\psi^{l,k}+\sum_{i=1}^{l}\sum_{j=1}^{l} a_{ij}(\psi^{l,k},\psi_i^0)\psi_j^0 = \lambda^{l,k}\psi^{l,k}. \tag{56}$$

Its solution is accomplished as follows:

If the eigenfunction $\psi^{l,k}$ is orthogonal to the span of $\{\psi_i^0\}_{i=1}^l$, equation (56) reduces to

$$[L^0-\gamma^*]\psi^{l,k} = \lambda^{l,k}\psi^{l,k} \tag{57}$$

which means that $L^{l,k}$ has the same eigenvalues and eigenfunctions as $[L^0-\gamma^*]$; or

$$\begin{aligned}\lambda_i^{l,k} &= \lambda_i^0-\gamma^* \\ \psi_i^{l,k} &= \psi_i^0\end{aligned} \qquad i > l. \tag{58}$$

If, however, $\psi^{l,k}$ is in the span of $\{\psi_i^0\}_{i=1}^l$, it may be written as

$$\psi^{l,k} = \sum_{n=1}^{l} \beta_n\psi_n^0 \tag{59}$$

Substitution in equation (56) yields

$$\sum_{i=1}^{l} \beta_i(\lambda_i^0-\gamma^*)\psi_i^0+\sum_{i=1}^{l}\sum_{j=1}^{l} a_{ij}\beta_j\psi_i^0 = \lambda^{l,k}\sum_{i=1}^{l}\beta_i\psi_i^0 \tag{60}$$

which in view of the linear independence of the eigenfunctions ψ_i^0 yields

$$\sum_{j=1}^{l}\{(\lambda_i^0-\gamma^*)\delta_{ij}+a_{ij}-\lambda^{l,k}\delta_{ij}\}\beta_j = 0 \qquad i = 1,2,\ldots l. \tag{61}$$

For non-trivial eigenfunctions $\psi^{l,k}$, the determinant of this system of equations must vanish:

$$\det|(\lambda_i^0-\gamma^*)\delta_{ij}+a_{ij}-\lambda^{l,k}\delta_{ij}| = 0. \tag{62}$$

This characteristic equation gives the eigenvalues of $L^{l,k}$ corresponding to the eigenfunctions in the span of $\{\psi_i^0\}_{i=1}^l$. These can then be ordered with the other eigenvalues obtained from equation (58).

The major labor involved in the determination of the eigenvalues $\lambda^{l,k}$ lies in the computation of the elements a_{ij}. From Bazley and Fox [16] and Fauconneau [17] we find that they can be computed from the equation

$$[a_{ij}] = \left[\frac{1}{\gamma^*}\left\{\delta_{ij}-\sum\frac{\lambda'_m}{\lambda'_m+\gamma^*}(\psi_i^0,\psi'_m)(\psi_j^0,\psi'_m)\right\}\right]^{-1}. \tag{63}$$

The positive parameter γ^* appearing in the formation of $L^{l,k}$ has been shown in Ref. [16] to have an optimum value for the determination of $\lambda_j^{l,k}$ such that $\lambda_{l+1}^0-\gamma^* = \lambda_j^{l,k}$. Since $\lambda_j^{l,k}$ is not known, γ^* must be chosen from an estimate of $\lambda_j^{l,k}$. Such an estimate was supplied here by the Rayleigh–Ritz procedure.

In the following section, the details of the numerical procedure used are reviewed, and the results are presented and discussed.

4. RESULTS AND DISCUSSION

The procedure used in the calculation of the eigenvalues of the plate was as follows: for a given aspect ratio a/b, and for given values of the parameters α and γ, the bounds for the eigenvalues λ defined by equation (12) were computed for fixed values of the parameter n. This parameter indicates the number of half waves in the mode shape in the y-direction. The range of discrete values of n considered was from 1 to 5. The circular frequencies were then calculated using equation (5).

The upper bounds were computed using 15×15 matrix sizes, and the lower bounds were obtained from intermediate operators with $k = l = 8$. Thus, for fixed aspect ratio and fixed loading, a sequence of eigenvalue problems (one for each value of n) was solved to take into account the possible combinations of half waves in the x- and y-directions giving the mode shapes of the plate. Consequently, for each case considered, the upper bound method yielded a matrix giving upper approximations to the eigenvalues of the plate for combinations of its first 5 half waves in the y-direction and its first 15 half waves in the x-direction. Similarly, the Second Projection method yielded lower approximations to the eigenvalues of the plate for combinations of its first 5 half waves in the y-direction and its first 8 half-waves in the x-direction. By inspection of the two resulting matrices, it was then possible to order the bounds to the eigenvalues in ascending order of magnitude, and to observe their corresponding mode orders.

This procedure was followed for fixed values of the parameter α and increasing values of γ to that value of γ for which the lowest eigenvalue became equal to zero. This critical value of γ gives an indication of the reduction of the critical constant edge loading brought about by the distributed in-plane load of magnitude corresponding to the given value of α.

The following geometrical and loading conditions were considered: $a/b = 0{\cdot}5$ for a range of α from 5·0 to 30·0; $a/b = 1{\cdot}0$ for α ranging from 5·0 to 65·0; $a/b = 2{\cdot}0$ for α ranging from 5·0 to 60·0 and $a/b = 3{\cdot}0$ for α ranging from 5·0 to 60·0.

The effect of the in-plane loads on the two lowest natural frequencies of the plate is illustrated in Figs. 2–9 for the various aspect ratios and loading conditions studied.

Examination of the figures indicates that the variation of the frequencies with the loading depends markedly on the aspect ratio of the plate. Two distinct types of behavior are evidenced, depending on whether the aspect ratio is less than or greater than 1·0.

1. *Aspect ratio less or equal to* 1·0

As illustrated in Figs. 2–5, for $a/b \leq 1{\cdot}0$, the natural frequencies decrease linearly with increasing values of γ, i.e. with increasing values of the edge loads, for fixed values of the distributed in-plane load parameter α. This rate of decrease is approximately constant for each frequency associated with a specific aspect ratio. It should be noted that in Figs. 3 and 5, which represent the variation of the second natural frequencies, the curves have been terminated at those values of γ for which the plate became elastically unstable.

For plates with aspect ratios 0·5 and 1·0, the lowest frequency always corresponds to the (1, 1) mode which is also the buckling mode of the plate.

The large effect of the distributed in-plane load on the frequency variations and on the critical values of the edge load parameter γ is illustrated by the wide spread between the curves corresponding to fixed values of the parameter α.

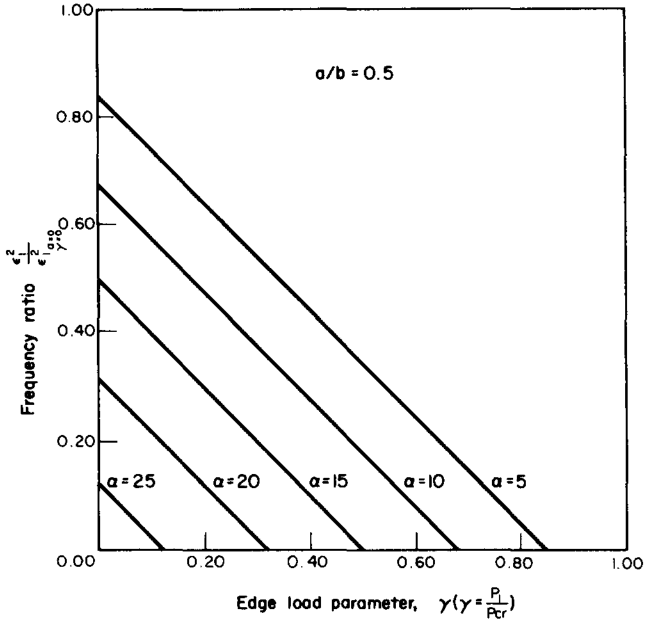

FIG. 2. First frequency variation with in-plane loads (aspect ratio = 0·5).

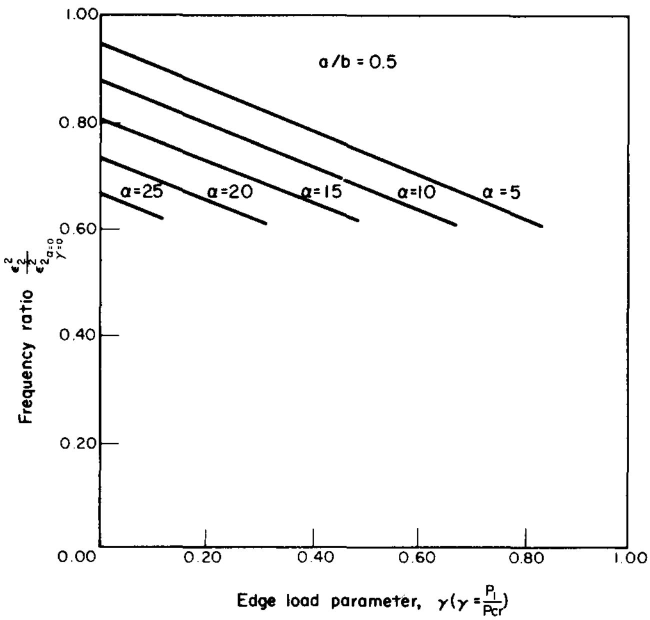

FIG. 3. Second frequency variation with in-plane loads (aspect ratio = 0·5).

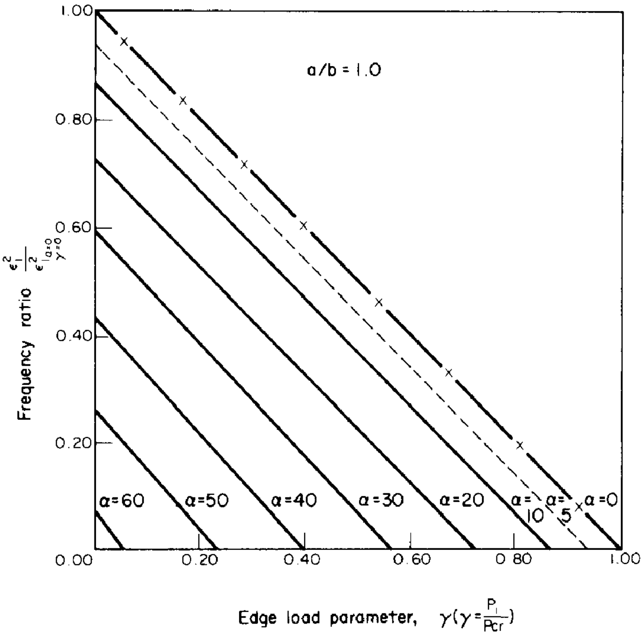

FIG. 4. First frequency variation with in-plane loads (aspect ratio = 1·0).

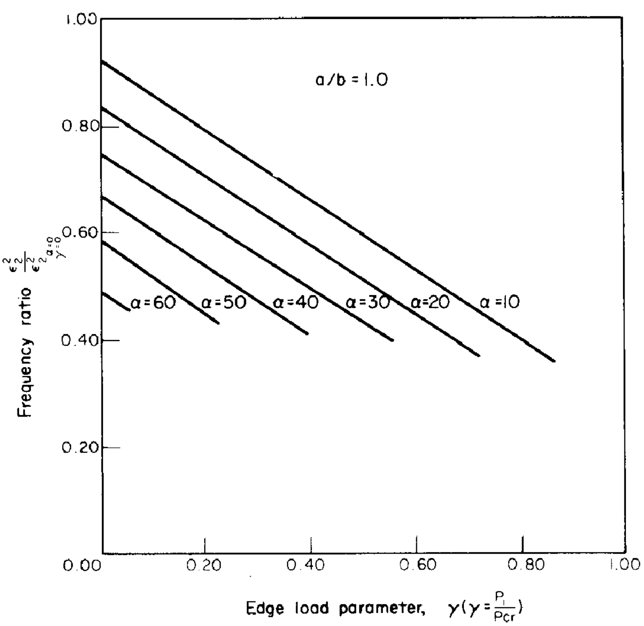

FIG. 5. Second frequency variation with in-plane loads (aspect ratio = 1·0).

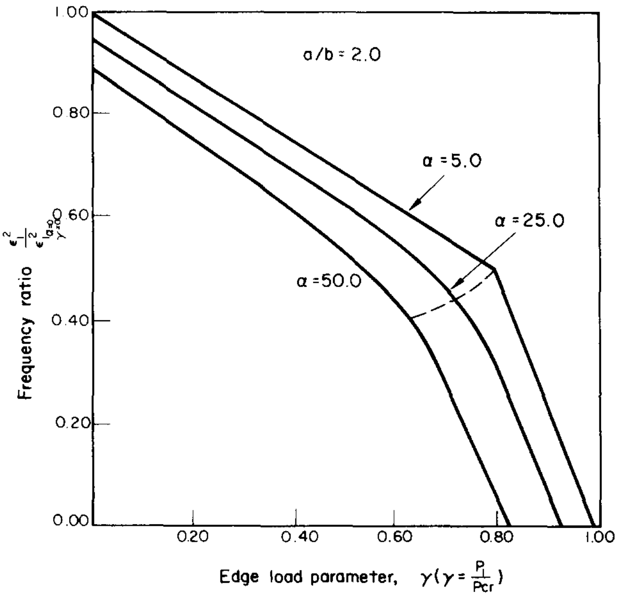

FIG. 6. First frequency variation with in-plane loads (aspect ratio = 2·0).

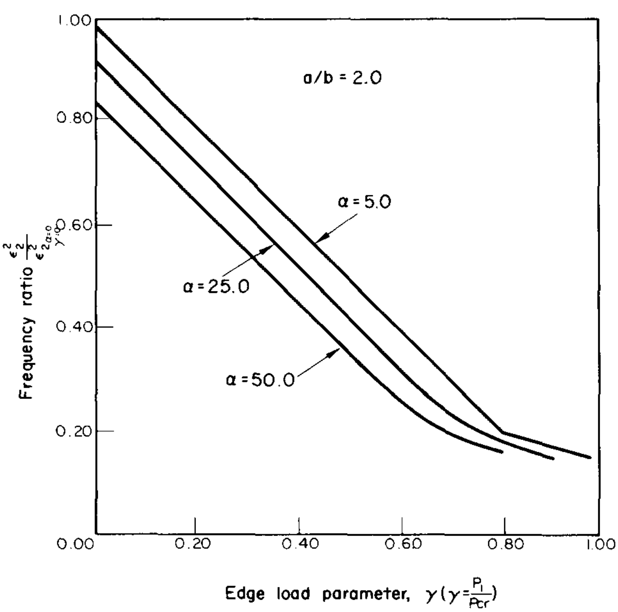

FIG. 7. Second frequency variation with in-plane loads (aspect ratio = 2·0).

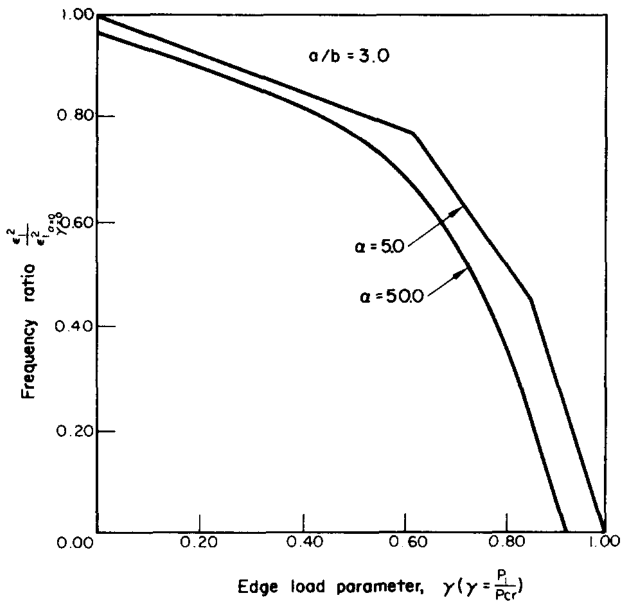

FIG. 8. First frequency variation with in-plane loads (aspect ratio = 3·0).

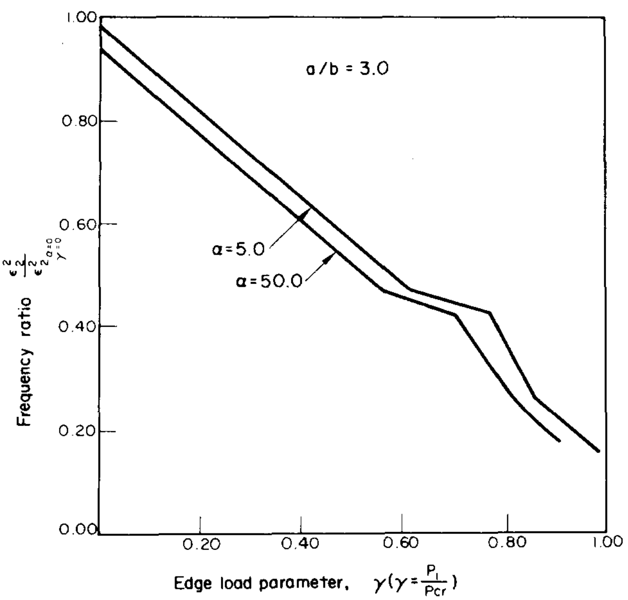

FIG. 9. Second frequency variation with in-plane loads (aspect ratio = 3·0).

2. *Aspect ratio greater than* 1·0

For aspect ratios greater than 1·0, the frequency variations with the loads are markedly different than those exhibited by plates with aspect ratios less than or equal to 1·0. Figures 6–9 illustrate the variations of the first two frequencies of plates with $a/b = 2{\cdot}0$ and 3·0. As the graphs indicate, the mode (1, 1) is not always the one corresponding to the lowest frequency of the plate. Indeed, for small values of γ the first mode of vibration is the (1, 1) mode and the frequency variation is essentially linear for γ up to approximately 0·5. However, as γ increases beyond this value, the lowest frequency switches to another mode. Figure 10 illustrates this phenomenon for a plate with $a/b = 2{\cdot}0$ and $\alpha = 50$. In that figure, the variations of the frequencies associated with the (1, 1) mode and the (2, 1) mode are illustrated. For γ less than 0·64, the lowest frequency is associated with the (1, 1) mode, and it decreases with increasing values of γ. The frequency associated with the (2, 1) mode also decreases with increasing values of γ. However, at $\gamma = 0{\cdot}64$, the two modes exchange roles: the lowest frequency now corresponds to the (2, 1) mode which eventually becomes the buckling mode as γ reaches its critical value. It should be noted that after this mode interchange, each one continues the variation trend initiated by the other one. The dashed line in Fig. 6 indicates the locus of the mode transition points for the various values of α plotted.

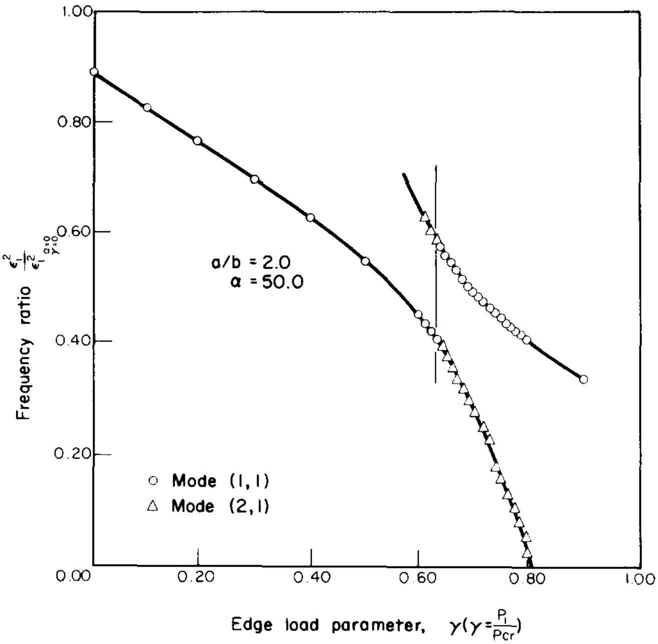

FIG. 10. Mode shift in the first frequency variation of a plate subjected to in-plane loads (aspect ratio = 2·0).

Figure 11 shows how the plate with $a/b = 3{\cdot}0$ exhibits two such mode shifts. First, the lowest frequency corresponds to the (1, 1) mode, then it switches to the (2, 1) mode and, eventually, to the (3, 1) mode which is then the buckling mode. Qualitatively, similar behaviors are exhibited by the higher order frequencies. For instance, in Fig. 9, the second frequency for the plate with $a/b = 3{\cdot}0$ shifts mode three times before buckling occurs.

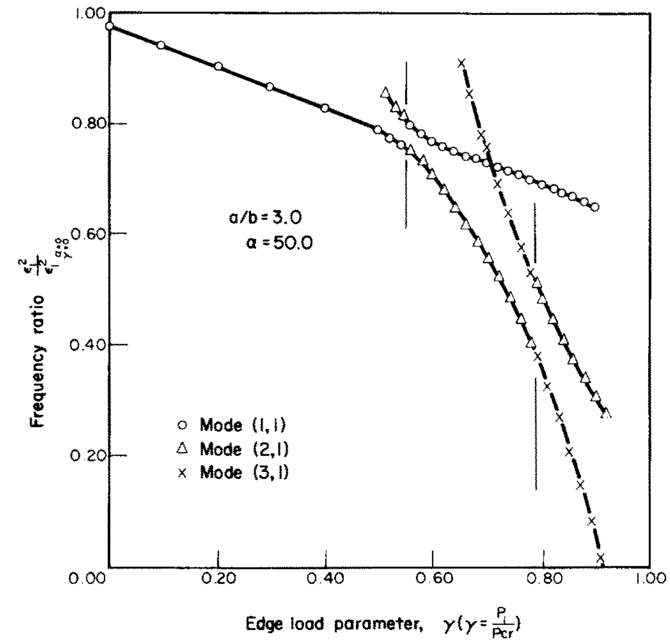

FIG. 11. Mode shift in the first frequency variation of a plate subjected to in-plane loads (aspect ratio = 3·0).

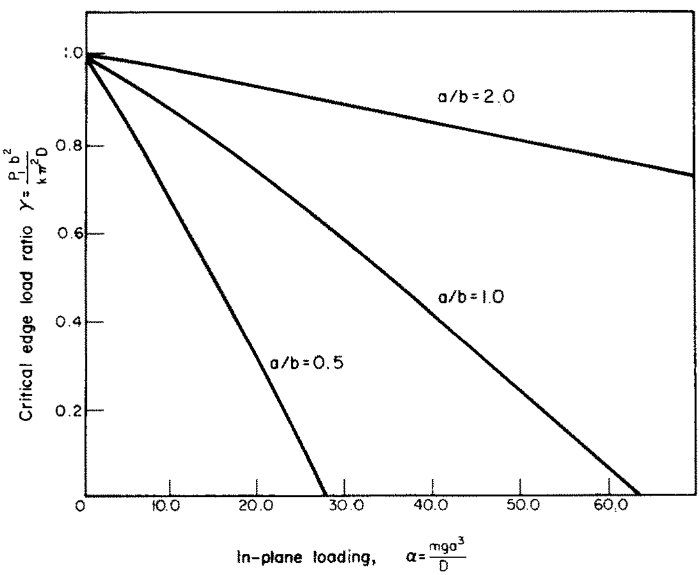

FIG. 12. Critical load buckling ratios.

Similar behaviors are to be expected for plates with higher aspect ratios. These results appear to be in qualitative agreement with the case handled by Herrmann [15] for $a/b = 3{\cdot}0$.

As illustrated by Figs. 6 and 8, the distributed in-plane load appears to have a much smaller effect on plates with a/b greater than 1·0 than on plates with aspect ratios less than or equal to 1·0.

TABLE 1. UPPER AND LOWER BOUNDS TO THE FREQUENCIES OF A SQUARE PLATE WITH COMPRESSIVE AND IN-PLANE LOADING, $\alpha = 10.0$

γ	Order	Upper bound	Lower bound
	1	339·24	339·21
	2	2236·66	2236·41
0·00	3	2385·33	2385·31
	4	6035·76	6035·52
	5	9295·64	9292·32
	1	300·29	300·18
	2	2080·81	2080·57
0·10	3	2346·35	2346·31
	4	5879·89	5879·65
	5	8944·98	8941·66
	1	261·17	261·14
	2	1924·97	1924·73
0·20	3	2307·37	2307·34
	4	5724·02	5723·78
	5	8594·32	8591·00
	1	222·11	222·08
	2	1769·13	1768·89
0·30	3	2268·38	2268·36
	4	5568·15	5567·92
	5	8243·66	8240·35
	1	183·05	183·02
	2	1613·30	1613·08
0·40	3	2229·40	2229·37
	4	5412·29	5412·04
	5	7893·01	7889·72
	1	143·96	143·93
	2	1457·49	1457·26
0·50	3	2190·41	2190·38
	4	5256·42	5256·18
	5	7542·36	7539·06
	1	104·85	104·81
	2	1301·70	1301·47
0·60	3	2151·42	2151·40
	4	5100·55	5100·32
	5	7191·71	7188·43
	1	65·71	65·68
	2	1145·94	1145·70
0·70	3	2112·43	2112·40
	4	4944·69	4944·44
	5	6841·07	6837·79
	1	26·52	26·50
	2	990·21	989·97
0·80	3	2073·44	2073·41
	4	4788·82	4788·57
	5	6490·43	6487·15

The effect of the distributed load on the critical edge load is illustrated in Fig. 12 which permits the determination of the critical edge load for a given value of the aspect ratio and of the distributed in-plane load parameter. The results obtained here compare favorably with those of Wang and Sussman [8]. For instance, for a square plate with $\gamma = 0$, the present study indicates that the value of α for buckling is equal to 63·8. Using the graphical results of Wang and Sussman for the same conditions, the critical value of α is calculated to be 64·15 (within the limits of accuracy of their graph).

The coupling of the Second Projection method with the Rayleigh–Ritz method yielded excellent results: in all instances, even near buckling, the gap between the bounds for the eigenvalues over their average was less than 0·5 per cent. Table 1 shows some of the numerical results for the bounds for the eigenvalues of a square plate. (Complete tabulated results are presented in Ref. 23.) The results show once more the quality of the Rayleigh–Ritz method (at least for the trial functions used in this application). Of course, this quality could not be established *a priori*, and only through the calculation of lower bounds can confidence be established to use the method in predicting the natural frequencies of plates with other aspect ratios and other values of the loading parameters.

Finally, it should be noted that one of the advantages in the methods used here resides in the fact that the shift in the modes of vibration is extremely easy to observe. In other methods, such as finite difference methods and finite element methods, such observations are rather difficult, if not impossible, to make.

Acknowledgements—The authors want to express their gratitude to Mr. William George for his assistance in the numerical calculations.

Parts of this study were supported by the National Aeronautics and Space Administration through Grant NSG 634.

REFERENCES

[1] W. G. BICKLEY, Deflexions and vibrations of a circular elastic plate under tension. *Phil. Mag.* **15**, 776–797 (1933).
[2] H. D. CONWAY, Bending of rectangular plates subjected to a uniformly distributed lateral load and to tensile or compressive forces in the plane of the plate. *J. appl. Mech.* **16**, 301–309 (1949).
[3] R. F. MORSE and H. D. CONWAY, The rectangular plate subjected to hydrostatic tension and to uniformly distributed lateral load. *J. appl. Mech.* **18**, 209–210 (1951).
[4] C. C. CHANG and H. D. CONWAY, The Marcus method applied to solution of uniformly loaded and clamped rectangular plate subjected to forces in its plane. *J. appl. Mech.* **19**, 179–184 (1952).
[5] M. STEIN and J. NEFF, Buckling Stresses of Simply Supported Rectangular Flat Plates in Shear, NASA Technical Note 1222 (1947).
[6] K. I. MCKENZIE, The buckling of a rectangular plate under combined biaxial compression, bending and shear. *Aeronaut. Q.* **15**, 239–246 (1964).
[7] D. J. JOHNS, Static Instability of Rectangular Orthotropic Panels Subjected to Uniform In-plane Loads and Deflection-Dependent Lateral Loads, Aeronautical Research Council Report A.R.C. 29281 (1967).
[8] T. M. WANG and J. M. SUSSMAN, Elastic stability of a simply supported plate under linearly variable compressive stresses. *AIAA Jnl* **5**, 1362–1364 (1967).
[9] G. E. WEEKS and J. L. SHIDELER, Effect of Edge Loadings on the Vibration of Rectangular Plates with Various Boundary Conditions, NASA TN D-2815 (1965).
[10] G. GERARD and H. BECKER, Handbook of Structural Stability, Part I. Buckling of Flat Plates, NACA TN 3781 (1957).
[11] S. P. TIMOSHENKO and J. M. GERE, *Theory of Elastic Stability*. McGraw-Hill (1961).
[12] W. NOWACKI, *Dynamics of Elastic Systems*. John Wiley (1963).
[13] L. S. D. MORLEY, *Skew Plates and Structures*. Macmillan (1963).
[14] J. E. ASHTON, Stability of clamped skew plates under combined loads. *J. appl. Mech.* **36**, 139–140 (1969).
[15] G. HERRMANN, The influence of initial stress on the dynamic behavior of elastic and viscoelastic plates. *Int. Ass. Bridges Struct. Engng Publ.* **15**, 275–294 (1956).

[16] N. W. BAZLEY and D. W. FOX, A procedure for estimating eigenvalues. *J. math. Phys.* **3**, 469–471 (1962).
[17] G. FAUCONNEAU, Upper and Lower Bounds for the Eigenvalues of Simply Supported and Clamped Uniform Beams Carrying Linearly Varying Axial Loads, Ph.D. Dissertation, Department of Mechanical Engineering, University of Pittsburgh (1966).
[18] R. COURANT and D. HILBERT, *Methods of Mathematical Physics*. Interscience (1953).
[19] J. B. DIAZ, Upper and lower bounds for eigenvalues. *Proc. Symp. appl. Math.* **8**, 53–78 (1959).
[20] S. H. GOULD, *Variational Methods for Eigenvalue Problems*. University of Toronto Press (1957).
[21] G. FICHERA, *Approximation and Estimates for Eigenvalues in Numerical Solution of Partial Differential Equations*, edited by J. H. BRAMBLE, pp. 317–352. Academic Press (1966).
[22] D. W. FOX and W. C. RHEINBOLDT, Computational methods for determining lower bounds for eigenvalues of operators in Hilbert space. *SIAM Rev.* **8**, 427–462 (1966).
[23] G. FAUCONNEAU and R. D. MARANGONI, Bounds for the Eigenvalues of a Simply Supported Rectangular Plate Under a Compressive Stress Varying Linearly in the Direction of Loading, Space Research Coordination Center Report, No. 116, University of Pittsburgh, Pittsburgh, Pa. (1969).

(*Received* 12 *February* 1970; *revised* 14 *August* 1970)

Абстракт—Исследуются эффекты постоянных краевых нагрузок и равномерно расположенных в плоскости нагрузок на частоты поперечных колебаний и характеристики упругой устойчивости свободно опертых пластинок. Получаются пределы собственных значений для разных отношении ширины пластинки к ее длине, в виде функций двух параметров, связанных с расположенной в плоскости нагрузкой и краевыми нагрузками. Определяется верхний предел методом Релея—Ритца, а нижний предел методом второй проекции Базлея и фокса. Для всех случаев, интервал между пределами, выше их средних значений, оказывается меньше чем половина процента. Получаются комбинации нагрузки выпучивания путем определения значении параметров нагрузки, которые сводят первые собственные значения к нулю.